ELSEVIER

Polymer 42 (2001) 3249–3257

polymer

www.elsevier.nl/locate/polymer

Synthesis and phase transition of liquid crystalline homopoly(ester–imide) and copoly(ester–imide)s with different lengths of methylene spacers

S.O. Kim, B.H. Jeon, I.J. Chung*

Department of Chemical Engineering, Korea Advanced Institute of Science and Technology, 373-1 Kusong, Yusong, Taejon 305-701, South Korea

Received 9 March 2000; received in revised form 12 June 2000; accepted 28 June 2000

Abstract

A homopoly(ester–imide) was prepared from *N*-(10-carboxydecanyl) trimellitic imide and hydroquinone diacetate via melt transesterification condensation. The phase transition behavior was checked with DSC, rheometry, and polarized light microscopy experiments. The homopoly(ester–imide) showed only crystallization transition when it was cooled from isotropic melt. Nevertheless it showed thread-like texture when quenched below crystallization temperature. In order to check mesophase formation, copoly(ester–imide)s containing both 10 and 4 methylene units were made varying the mole ratio of *N*-(10-carboxydecanyl) trimellitic imide to *N*-(4-carboxybutyl) trimellitic imide. All copoly(ester–imide)s exhibited nematic phase transition and, in particular, they showed monotropic nematic transition, when they had large portion of 10 methylene unit. The nematic to isotropic phase transition temperature of homopoly(ester–imide) was obtained extrapolating those of copoly(ester–imide)s and matched well with the crystallization temperature of the homopoly(ester–imide). © 2001 Published by Elsevier Science Ltd.

Keywords: Poly(ester–imide); Phase transition; Rheological properties

1. Introduction

Polyimides have attracted much attention due to their high thermal stability, good mechanical and electrical properties [1]. However, the difficulty in processing, caused by poor flow properties and infusibility, has restricted their application. The synthesis of poly(ester–imide)s was motivated to resolve such problems [2]. The introduction of flexible ester linkage may lower processing temperature and improve the flow property at the expense of the thermal stability. In addition, a lot of poly(ester–imide)s have been reported to show liquid crystalline phases [3].

Although most of the imide moieties have been reported not to have mesogenic characters, various synthesized poly(ester–imide)s showed liquid crystalline properties [3]. Typical examples are fully aromatic poly(ester–imide)s with nematic phase[4,5] and semiflexible poly(ester–imide)s [6–13] with smectic phases. In particular, most of the semiflexible poly(ester–imide)s have been known to show smectic layer structure, which is attributed to regular sequence of molecular structure and the great polarity difference between aromatic units including imide linkage and methylene spacers [6–13].

Several thermotropic poly(ester–imide)s have been synthesized by our group [14,15]. Various nematic type liquid crystalline poly(ester–imide)s were obtained with the asymmetric structure of *N*-(ω-carboxyalkylene) trimellitic imide monomer. In the present study, *N*-(10-carboxydecanyl) trimellitic imide and hydroquinone diacetate were used to synthesize a homopoly(ester–imide). Besides copoly(ester–imide)s were synthesized adding another imide containing monomer, *N*-(4-carboxybutyl) trimellitic imide. The mole ratio of *N*-(10-carboxydecanyl) trimellitic imide to *N*-(4-carboxybutyl) trimellitic imide was varied and the phase transition behaviors were observed. The copolymers with methylene spacers of different lengths have been reported to show extremely suppressed crystallization behaviors [15,16]. Sometimes the mesophase of semiflexible liquid crystalline polymer, which is hidden below crystallization transition, appears with the copolymerization [17–20]. It should be noted that the poly(ester–imide) derived from *N*-(10-carboxydecanyl) trimellitic imide and hydroquinone was already synthesized by Kricheldorf et al. [21]. But they did not inform the precise phase transition behaviors.

* Corresponding author. Tel.: +82-42-869-3916; fax: +82-42-869-3910.
E-mail address: chung@cais.kaist.ac.kr (I.J. Chung).

0032-3861/01/$ - see front matter © 2001 Published by Elsevier Science Ltd.
PII: S0032-3861(00)00540-1

Table 1
Abbreviation and inherent viscosity values of poly(ester–imide) and copoly(ester–imide)s

Abbreviation	T10/T4 mole ratio	Inherent viscosity[a] (dl/g)
10H	Homopolymer (10/0)	0.28
9C	9/1	0.30
8C	8/2	0.25
7C	7/3	0.29
6C	6/4	0.23
5C	5/5	0.27
4C	4/6	0.20
3C	3/7	0.29
2C	2/8	0.26
1C	1/9	0.21

[a] Measured in *m*-cresol at the concentration of 0.5 g/dl at 20°C.

2. Experimental

2.1. Materials and polymerization

Trimellitic anhydride, 5-aminovaleric acid, 11-aminoundecanoic acid, and hydroquinone were purchased from Aldrich Chemical Co. Hydroquinone was acetylated by means of acetic anhydride in boiling toluene with the catalytic amount of pyridine. *N*-(4-carboxybutyl) trimellitic imide (T4) and *N*-(10-carboxydecanyl) trimellitic imide (T10) were prepared from ω-amino acids and trimellitic anhydride via chemical imidization in DMF with toluene. Polymerization scheme of poly(ester–imide) and copoly(ester–imide)s was the same with that of our previous publication [14]. The chemical structures of the all prepared poly(ester–imide) and copoly(ester–imide)s are shown below. Abbreviations and inherent viscosity values are summarized in Table 1. It has to be noted that the poly(ester–imde), 10H, has random copolymeric character due to the unsymmetric chemical structure of T10 [14]. In this article, 10H is referred as a homopolymer in the meaning that it is constituted with one kind of aliphatic spacer, 10 methylene unit. In contrasts, the poly(ester–imide)s containing both 4 and 10 methylene units are referred as copolymers.

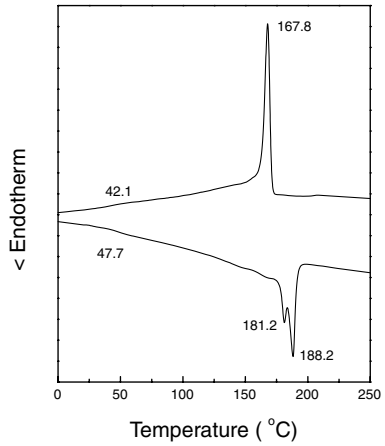

Fig. 1. DSC cooling and subsequent heating scans of poly(ester–imide), 10H at scan rates of 10°C/min.

2.2. Measurements

Inherent viscosities of poly(ester–imide) and copoly(ester–imide)s were measured in *m*-cresol at the concentration of 0.5 g/dl at 20°C. A polarized light microscope (PLM, A Leitz, Model Laborlux 12 Pols) coupled with a Mettler FP-2 hot stage was used to observe the morphology change. Thermal transition experiments were carried out with du Pont 2010 Thermal Analyzer and Penkin Elmer DSC 7 under nitrogen atmosphere. Wide angle X-ray diffractograms (WAXD) were obtained using Rigaku X-ray generator ($CuK\alpha_1$ radiation with $\lambda = 0.1540$ nm) with the scan speed of 2°/min. Temperature sweep measurements of viscoelastic properties were conducted with PHYSICA RheoLab MC 120 rheometer. 5 mm parallel plate was used. Samples were molded into disk shape and dried sufficiently before measurements.

3. Results and discussion

3.1. Phase transition behavior of poly(ester–imide) containing 10 methylene units

Fig. 1 shows the DSC cooling and subsequent heating scans of the poly(ester–imide), 10H. Upon cooling at a rate of 10°C/min, one exotherm at 167.8°C and a weak glass transition at 42.1°C appear. The heating scan at the same rate exhibits a glass transition at 47.7°C and two endotherms at 181.2 and 188.2°C. The heat generated for the exotherm on cooling (4.6 kcal/mru) matches well with

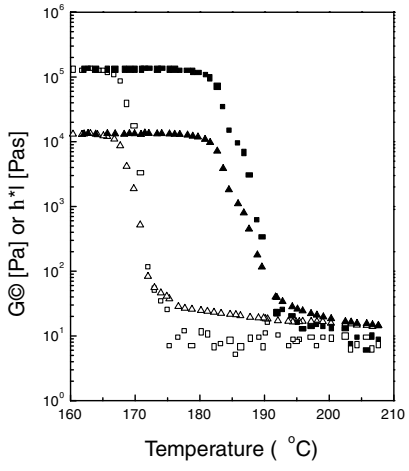

Fig. 2. Temperature scans of viscoelastic properties of 10H at scan rates of 10°C/min: □, G'; and △, $|\eta^*|$. The open symbols stand for cooling and the closed symbols for heating. The cooling scans were conducted first and the heating scan followed immediately. $\omega = 1$ rad/s and $\gamma = 0.1$.

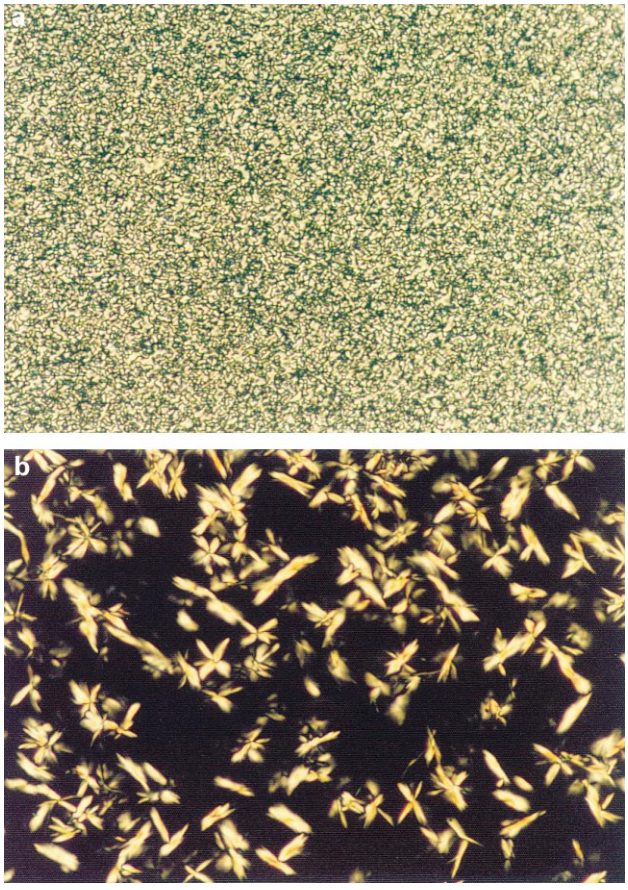

Fig. 3. Polarized light micrographs of 10H: (a) air-quenched from isotropic melt, (b) cooled from isotropic melt to 175°C at a rate of 15°C/min and then isothermally annealed for 1 min.

total heat for two endotherms on heating. The viscoelastic properties at the thermal transitions are checked with rheological temperature sweep measurements. The results are shown in Fig. 2. The cooling scan was conducted first. The scan rates were 10°C/min, the same with those of DSC. The elastic modulus and complex viscosity increase abruptly around 170°C on cooling. Upon heating they keep the high values up to nearly 185°C and then decrease rapidly to the initial values of cooling scan above 190°C. The change on the cooling scan corresponds to the crystallization transition and the change on heating indicates the melting transition [14,15,22,23].

Despite the fact that DSC and rheological measurements showed only crystallization and melting transitions, the texture evolution under polarized light microscopy shows extraordinary features. When a sample is quenched below 165°C from isotropic melt, a thread-like texture appears (Fig. 3(a)). After the texture formation, the sample does not show any flow property when the cover glass is pulled. When the sample is reheated above 185°C, it becomes isotropic. On the contrary, when it is annealed above 168°C, it exhibits completely different morphology evolution. As the annealing continues, anisotropic spots appear and grow to form axialites in dark background, which demonstrates the typical nucleation and growth mechanism of polymer crystallization. Fig. 3(b) shows the micrographs taken for the sample isothermally annealed at 175°C for 1 min. The distinct difference of morphology evolution has been reported for monotropic liquid crystalline polymer [11–13,24–27]. But it is different from most of the monotropic liquid crystalline polymers that 10H does not show temporal flow property after mesophase formation. Nevertheless one can suggest the possibility that homopoly(ester–imide), 10H, should be a monotropic liquid crystalline polymer and it crystallizes simultaneously with the isotropic to mesophase transition.

Usually the crystallization of polymer can be easily delayed with fast cooling rates. Whereas, the low-ordered mesophase transitions follow near equilibrium state. So, the mesophase transition of a monotropic liquid crystalline polymer, which is obscured by crystallization, can be

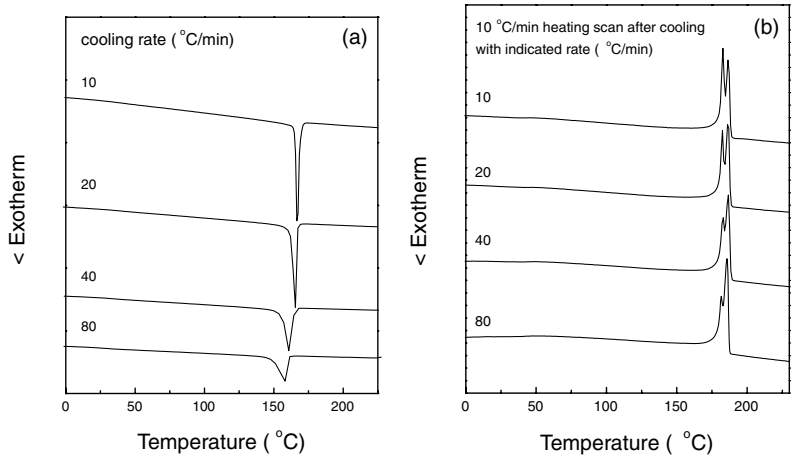

Fig. 4. DSC thermograms of 10H: (a) cooling scan from isotropic melt at various scan rates, (b) heating scans at a rate of 10°C/min after the cooling scans at indicated rates.

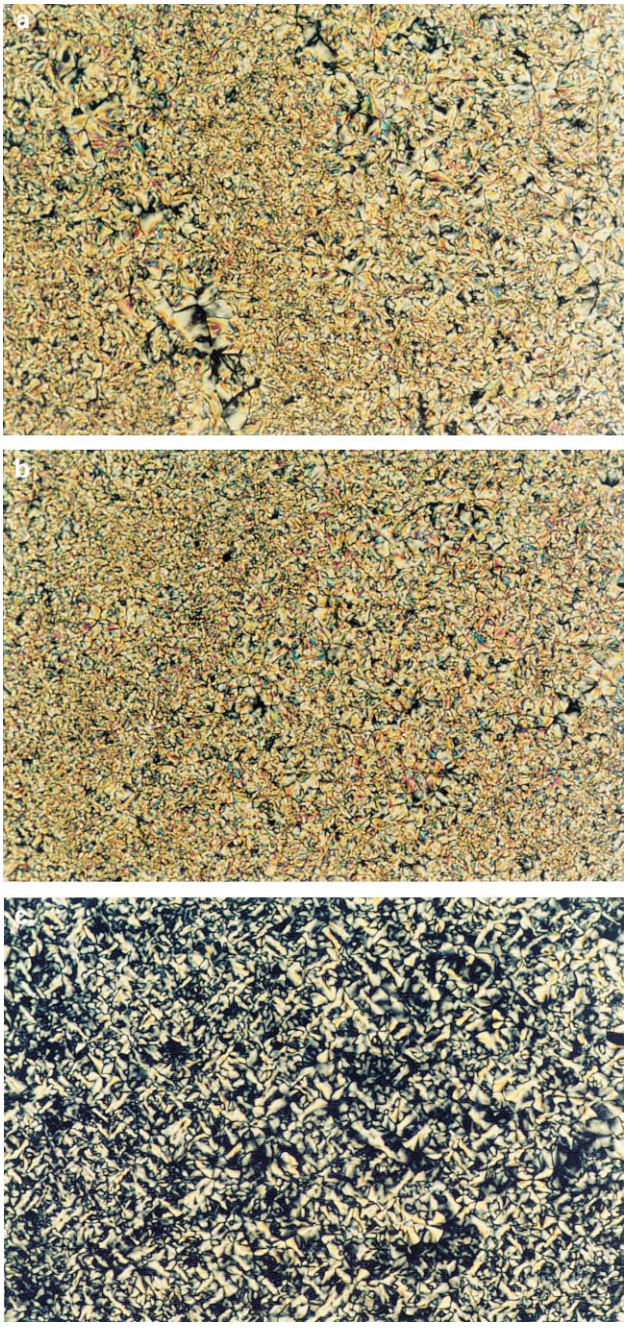

Fig. 5. Polarized light micrographs of 10H: (a) cooled from isotropic melt to 165°C at a rate of 10°C/min, (b) cooled from isotropic melt to 165°C at a rate of 20°C/min, and (c) the sample (b) heated to 185°C.

separated with fast cooling rates [10–13,24–32]. Fig. 4(a) shows the DSC thermograms measured at various cooling rates. Even at the highest cooling rate of 80°C/min, the isotropic to mesophase transition is not discernible. The noticeable feature is that the peak position of the exotherms shows little dependence on the cooling rates, compared with other semiflexible polymers [10]. The immediate heating with the scan rate of 10°C/min after each cooling scan shows the dual endotherms in Fig. 4(b).

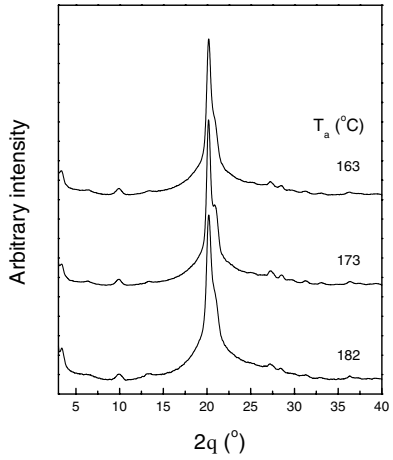

Fig. 6. WAXD diffractograms of 10H annealed at various temperatures until the completion of crystallization.

The total heat generated on heating is constant regardless of the cooling rate, but the heat generated for the peak at the high temperature becomes higher as the cooling rate increases.

To investigate the nature of the dual endotherms, the polarized light microscopy observation was carried out. Fig. 5(a) is the micrograph for a sample cooled from isotropic melt to 165°C at a rate of 10°C/min. One can find that both of thread-like and axialitic crystal morphologies coexist. Fig. 5(b) shows the micrographs taken after cooled from isotropic melt with a rate of 20°C/min. There are more threaded textures than the micrograph of Fig. 5(a). Fig. 5(c) is the micrographs taken for the same sample of Fig. 5(b), reheated to 185°C between the peak temperatures on DSC heating scan in Fig. 1. One can find that the spots of axialitic morphology of Fig. 5(b) darken first. This morphology change suggests that both crystallization and mesophase formation of the homopoly(ester–imide) might occur simultaneously and the higher temperature melting transition might correspond to the melting of the crystal formed from mesophase. Cheng and coworkers [31,33] reported similar crystallization behavior for a monotropic liquid crystalline polycarbonate. They noted that the nematic mesophase served as nucleus for crystallization and the crystal formed in mesophase was more perfect and melted at a higher melting temperature than that formed in isotropic phase. But they could observe the isotropic to nematic phase transition, which was separated from crystallization during cooling process.

Crystal structure change was checked with WAXD. Each sample was heated to be isotropic melt and immediately air-quenched to an annealing temperature. Isothermal annealing time was sufficiently long enough for the completion of crystallization. Fig. 6 shows the diffractograms for samples annealed at 163, 173 and 178°C, which are around the peak temperature of crystallization during DSC cooling scan. All diffractograms show almost the same peak pattern.

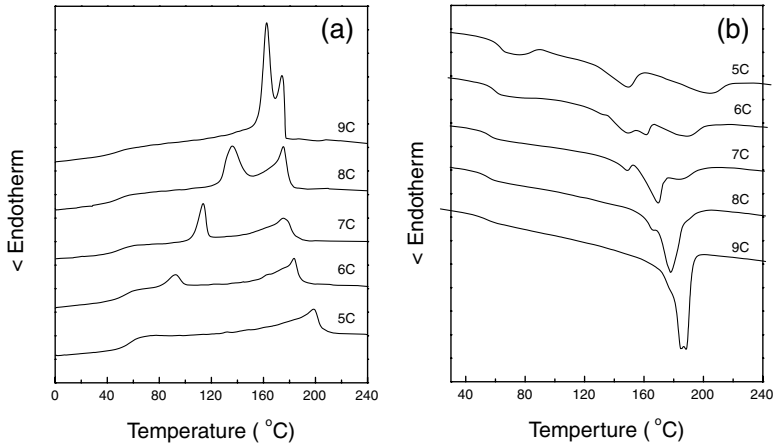

Fig. 7. DSC thermograms of copoly(ester–imide)s, 5C–9C: (a) cooling scans at a rate of 10°C/min, (b) subsequent heating scans at a rate of 10°C/min.

A major peak around 20° means a hexagonal lateral packing [14].

3.2. Phase transition behaviors of copoly(ester–imide)

It was recognized from the above results that homopoly(ester–imide), 10H, might be a monotropic liquid crystalline polymer. To clarify the phase transition behavior of 10H, a series of copoly(ester–imide)s were synthesized from *N*-(10-carboxydecanyl) trimellitic imide, *N*-(4-carboxybutyl) trimellitic imide, and hydroquinone diacetate. As mentioned in Section 1, the copolymerization of aliphatic spacers containing different numbers of methylene units has been used to check the mesophase transitions hidden by the crystallization [17–20]. It has been known that not only aromatic mesogenic unit but also methylene spacer unit participates in mesophase ordering and, therefore, the nematic to isotropic phase transition temperature depend linearly on the composition of methylene spacers [15,17–20]. The phase transition behavior of another homopoly(ester–imide) made from *N*-(4-carboxybutyl) trimellitic imide and hydroquinone diacetate was reported earlier by our group [14]. It showed the typical enantiotropic nematic phase transition.

Fig. 7 shows the DSC thermograms of 5C–9C on cooling and subsequent heating with the scan rate of 10°C/min. Each sample except 5C exhibit two exothermic transitions, as shown in Fig. 7(a). The temperature difference between two peaks becomes larger with the composition of *N*-(4-carboxybutyl) trimellitic imide. The polarized light microscopy observation revealed that when cooled from isotropic melt all polymers exhibited the thread-like morphology around the temperature of high temperature exotherm. The immediate heating scan curves are shown in Fig. 7(b). 5C–7C show the mesophase to isotropic phase transitions (biphasic morphology under polarized light microscopy) around the temperatures of the isotropic to mesophase transition on cooling scan. However, 8C and 9C do not show biphasic morphology and directly melt into isotropic melt.

Another interesting feature is that copoly(ester–imide)s, 6C–9C show multiple (dual or triple) melting endotherms as the case of homopoly(ester–imide), 10H (see Fig.1 and Fig. 4(b)). The multiple endothermic behavior of 10H was

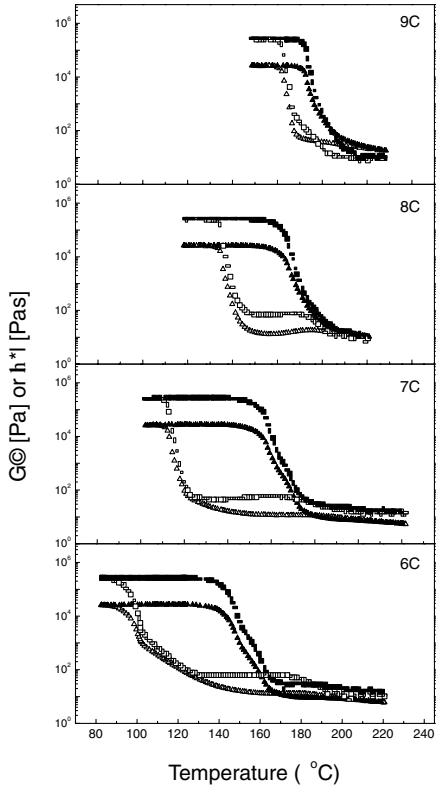

Fig. 8. Cooling and subsequent heating scans of viscoelastic properties for copoly(ester–imide)s at a scan rate of 10°C/min: □, G', and △, $|\eta^*|$. The open symbols stand for cooling and the closed symbols for heating. The cooling scans were conducted first and the heating scan followed immediately. $\omega = 1$ rad/s, $\gamma = 0.1$.

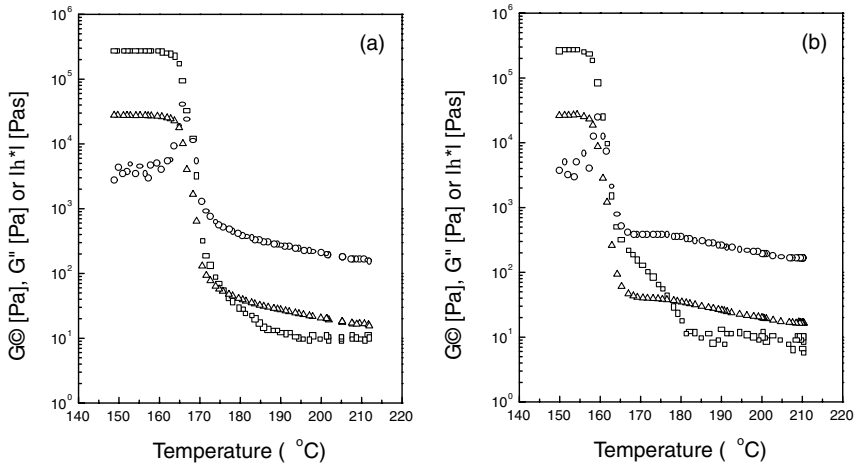

Fig. 9. Cooling scans of viscoelastic properties for copoly(ester–imide), 9C: (a) cooling rate of 5°C/min, (b) cooling rate of 15°C/min: □, G'; ○, G''; and △, $|\eta^*|$.

attributed to two kinds of crystal formation according to initial phase (mesophase or isotropic phase). Same behaviors are observed in the case of the monotropic liquid crystalline copoly(ester–imide)s, 8C and 9C, when they are cooled slowly from isotropic melt.

The phase transitions observed on DSC are verified by the temperature sweep measurements of viscoelastic properties. The scan rate was the same with the DSC experiments. Fig. 8 shows the results of elastic moduli and complex viscosities for 6C–9C. The copoly(ester–imide), 9C, show similar behavior with that of homopoly(ester–imide), 10H except a shoulder shape of loss modulus around 175°C on cooling scan. On cooling 8C shows peak shapes of the elastic modulus and complex viscosity around 165°C, which is a unique feature at the isotropic to nematic phase transition [22,34–39]. The cooling scans of 7C and 6C show similar peak shapes. But the temperature regions of transition are broader with the increase of *N*-(4-carboxybutyl) trimellitic imide composition. It should be noted that 7C exhibited the enantiotropic mesophase transition on DSC measurement and polarized light microscopy observation. But it is difficult to conform enantiotropic transition by the rheological method. This may be attributed to the significant temperature distribution in a large sample fixture of the rheological measurements. The heating scan of 6C shows similar peak shape to that on the cooling scan, which confirms a enantiotropic nematic to isotropic phase transition.

Fig. 9(a) and (b) show dynamic moduli and complex viscosities of 9C measured on cooling scan at scan rates of 5 and 15°C/min, respectively. Fig. 9(a) exhibit neither peak shape of moduli and complex viscosity of the isotropic to nematic phase transition nor the shoulder shape shown in the cooling result with the rate of 10°C/min (Fig. 8). But, in Fig. 9(b) the peak shape appears around 175°C, which agrees well with the first exothermic transition during DSC cooling scan shown in Fig. 7(a). From the rheological measurements one can find that the mesophase of all copoly(ester–imide)s are nematic and that 8C and 9C are monotropic liquid crystalline polymers.

Fig. 10 shows the polarized light micrographs of the monotropic liquid crystalline copoly(ester–imide)s, 8C and 9C. In Fig. 10(a) taken during cooling of 8C with 5°C/min, bright spots appear are around 166°C, which are nematic domains growing in the isotropic melts (Fig. 11(a)). At the lower temperature of 160°C, the entire sample gets anisotropy (Fig. 10(b)). Fig. 10(c) is the micrographs of 9C taken during isothermal annealing at 182°C, which is above the nematic to isotropic transition temperature, after cooling from isotropic melt. 9C shows the axialitic crystal growth like 10H. But the morphology evolution is slower than that of 10H due to its copolymeric character.

The transition temperatures of all copoly(ester–imide)s measured by DSC heating and cooling scans at rates of 10°C/min are summarized in Table 2. The glass transition temperature of copoly(ester–imide) decreases linearly with the composition of *N*-(10-carboxydecanyl) trimellitic imide. Most copolymers exhibit dual melting transitions. T_{m2}, is the major crystal melting transition temperature for each polymer. T_{m2} of 4C is the lowest. Fig. 11 shows the WAXD diffractograms of all copoly(ester–imide)s annealed sufficiently for the completion of crystallization. The copoly(ester–imide), 3C, shows the minimum crystallinity. Usually the great depression of crystallization occurs for the copolymer containing equal amount of each monomer unit. The highest depression of crystallization for 3C or 4C might be attributed to the higher crystallization rate of long methylene spacer in *N*-(10-carboxydecanyl) trimellitic imide unit [32].

One can find small angle peaks in the diffractograms of 7C–9C. As shown in Fig. 6, homopoly(ester–imide), 10, show similar peaks. The peak intensity grows as the composition of *N*-(10-carboxydecanyl) trimellitic imide increases. The small angle peaks are observed in smectic

type liquid crystalline polymers as the layer spacing of smectic structure. But the mesophase of 7C–9C are verified as nematic ones from rheological measurements. Thus, the small angle peaks might be attributed to the crystal structure of homopoly(ester–imide), 10H.

The phase diagram is plotted with the mole composition of *N*-(10-carboxydecanyl) trimellitic imide in Fig. 12.

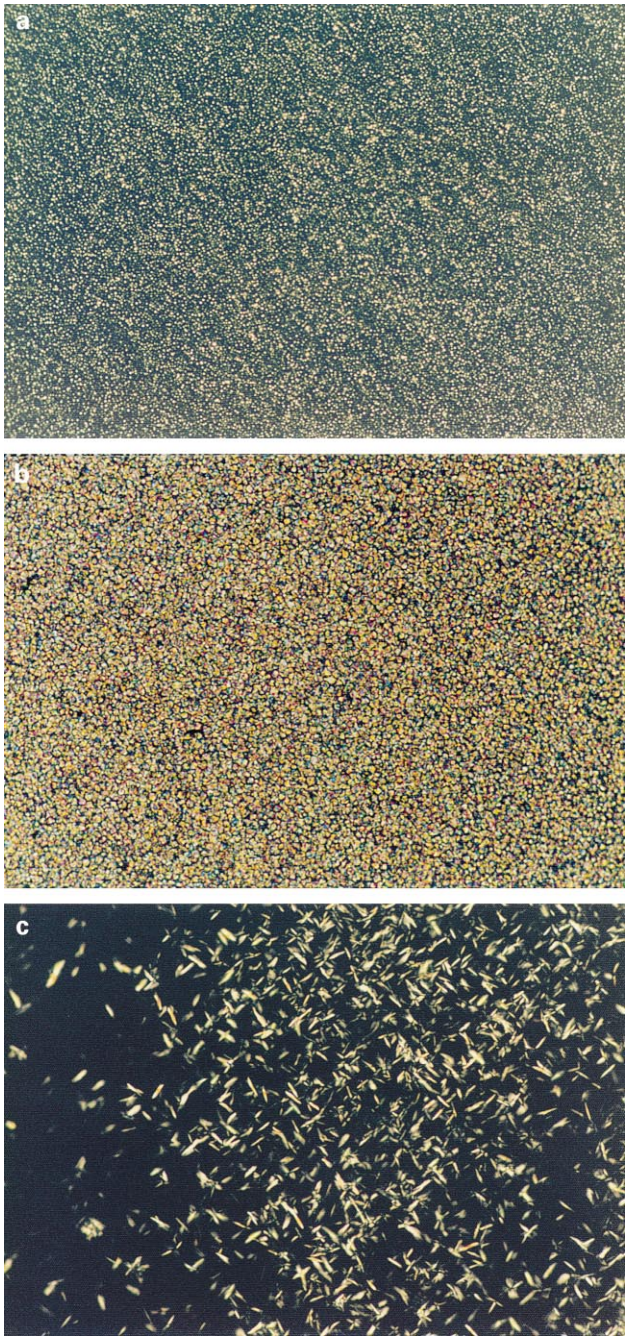

Fig. 10. Polarized light micrographs of copoly(ester–imide)s: (a) a photograph of 8C taken at 166°C during cooling at 5°C/min, (b) a photograph of 8C taken at 160°C during cooling at 5°C/min, (c) a photographs of 9C isothermally annealed at 182°C for 200 min after cooling from isotropic melt.

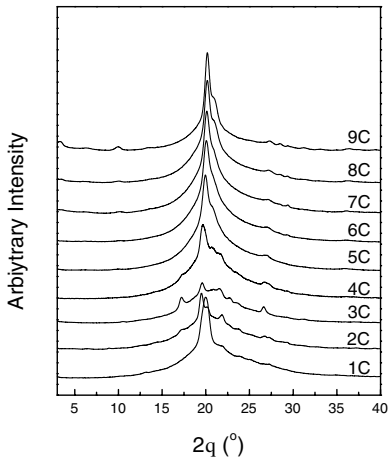

Fig. 11. WAXD diffractograms of copoly(ester–imide)s annealed around 30°C/min below the meting temperatures of each polymer until the completion of crystallization.

The glass transition and melting temperatures were obtained from DSC heating scans at the scan rate of 10°C/min and the nematic to isotropic phase transition temperatures were obtained from DSC cooling scans at the same rate. Both glass transition and isotropic to nematic phase transition depend linearly on the *N*-(10-carboxydecanyl) trimellitic imide composition. The isotropic to nematic phase transition temperature of 10H is obtained by extrapolating those of copoly(ester–imide)s. The value is approximately 162.9°C, matching well with the crystallization temperature of 10H during the cooling scan (Fig. 1). The result confirms that the homopoly(ester–imide), 10H, crystallize simultaneously

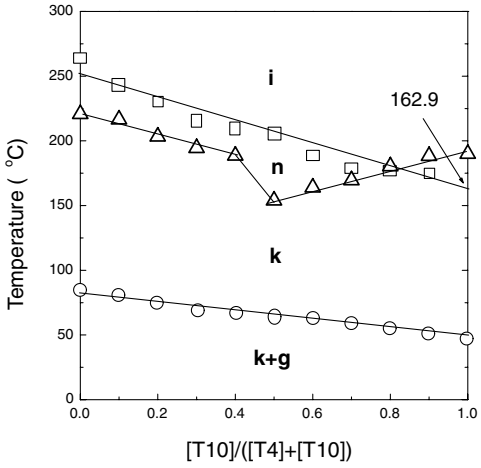

Fig. 12. Phase diagram of all poly(ester–imide)s with the variation of the mole composition of *N*-(10-carboxydecanyl) trimellitic imide: □, isotropic to nematic phase transition; △, melting temperature, and ○, glass transition temperature — i, isotropic; n, nematic; k, crystalline; g, nematic glassy phase. The glass transition and melting temperatures were obtained from DSC heating scan and the nematic to isotropic phase transition temperatures were obtained from DSC cooling scan.

with the isotropic to nematic phase transition. It has been generally accepted, in the studies on monotropic liquid crystalline polymers, that the crystallization rate is faster in mesophase than in isotropic phase [11,13,24,27,33,40,41]. The mechanism of crystallization acceleration is not known precisely, because it is hard to discern nucleation and crystal growth stage in mesophase. According to Cheng and coworker, mesophase can serve as the nuclei for crystallization [31,33]. From the earlier findings the unique phase transition behavior of 10H can be explained. The homopoly(ester–imide) does not crystallize in isotropic phase under usual cooling rate. But at the initiation of nematic phase formation, it starts to crystallize abruptly from the nematic domain. And the isotropic region crystallizes subsequently from the nuclei of crystals formed earlier.

Finally, the origin of monotropic type mesophase formation should be discussed. As reported earlier by our group, the homopoly(ester–imide)s made from *N*-(4-carboxybutyl) trimellitic imide and *N*-(6-carboxyhexyl) trimellitic imide with hydroquinone diacetate showed enantiotropic type mesophase. It has been reported that as the length of methylene spacer increase, the temperature region of mesophase decreases [10,12,42]. It was attributed to the difference of entropic and enthalpic contribution for mesophase formation between rigid mesogenic unit and flexible methylene unit. Because 4, 6, and 10 methylene spacer lengths are all even number, same generalization can be applicable in this case. In addition, the poly(ester–imde)s made from our group, contains the unsymmetric *N*-(ω-carboxyalkylene) trimellitic imide unit. As noted above, the monomer unit is a good material to synthesis semiflexible type nematic liquid crystalline polymer. However, its unsymmetric structure gives randomized molecular structure. Thus, one can suggest that the stability of mesophase order might be lower than that of usual mesogen-spacer type semiflexible liquid crystalline polymer.

4. Conclusions

A homopoly(ester–imide) was prepared from *N*-(10-carboxydecanyl) trimellitic imide, and hydroquinone diacetate. The homopoly(ester–imide) exhibited only a crystallization and corresponding melting transitions on DSC and rheological temperature sweep experiments. But after the quenching from isotropic melt to below the temperature of the crystallization exotherm, a thread-like texture of mesophase was observed. To verify whether homopoly(ester–imide) is a monotropic polymer, copoly(ester–imide)s containing both 4 and 10 methylene spacer are synthesized, varying the mole composition of *N*-(carboxydecalyl) trimellitic imide to *N*-(4-carboxybutyl) trimellitic imide, and their phase transition behaviors are checked. All copoly(ester–imide)s exhibited nematic mesophase. The copoly(ester–imide)s containing high composition of *N*-(10-carboxydecanyl) trimellitic imide showed monotropic mesophase, which was proved by DSC, polarized light microscopy, and rheological temperature sweep experiments. The nematic to isotropic phase transition temperature of homopoly(ester–imide) was extrapolated with those of copoly(ester–imide)s. It was about 162.9°C, which matches well with the crystallization temperature of 10H.

Acknowledgements

This work was financially supported by the Korea Science and Engineering Foundation, KOSEF, under contract 971-0804-039-2.

Table 2
The transition temperatures of copoly(ester–imide)s observed on DSC heating and cooling scans at a rate of 10°C/min

Polymer	Heating				Cooling		
	T_g[a] (°C)	T_{m1}[b] (°C)	T_{m2}[b] (°C)	T_i[c] (°C)	T_g[a] (°C)	T_c[d](°C)	T_i[c](°C)
9C	54.1	185.1	188.3	–	49.0	119.8	175.2
8C	54.9	171.2	180.4	–	50.1	–	177.3
7C	56.2	148.8	169.5	181.8	53.2	–	179.1
6C	59.3	153.7	164.0	191.0	55.3	–	189.4
5C	63.8	–	153.9	206.9	61.7	–	204.7
4C	68.4	159.0	188.6	214.2	66.6	–	210.0
3C	73.6	156.0	194.5	220.3	69.9	113.7	215.3
2C	74.2	196.4	203.3	234.7	71.8	136.3	230.5
1C	80.3	–	216.5	247.1	76.2	162.5	243.4

[a] Glass transition temperature.
[b] Melting temperature.
[c] Nematic to isotropic phase transition tempeature.
[d] Crystallization temperature.

References

[1] Mittal KL. Polyimides: synthesis, characterization and application. New York: Plenum, 1985.
[2] de Abajo J, de la Campa JG. Adv Polym Sci 1999;140:3–59.
[3] Kricheldorf HR. Adv Polym Sci 1999;141:83–188 (and references therein).
[4] Kricheldorf HR, Domschke A, Schwarz G. Macromolecules 1991;24:1011–6.
[5] Kricheldorf HR, Schwarz G, Domschke A, Linzer V. Macromolecules 1993;26:5161–8.
[6] Kricheldorf HR, Pakull R. Macromolecules 1988;21:551–7.
[7] Kricheldorf HR, Pakull R, Buchner S. Macromolecules 1988;21:1929–35.
[8] Kricheldorf HR, Probst N, Wutz C. Macromolecules 1995;28:7990–5.
[9] Kricheldorf HR, Schwarz G, Berghahn M, de Abajo J, de la Campa J. Macromolecules 1994;27:2540–7.
[10] Kricheldorf HR, Probst N, Schwarz G, Wutz C. Macromolecules 1996;29:4234–40.
[11] Pardey R, Zhang A, Gabori PA, Harris FW, Cheng SZD, Adduci J, Facinelli JV, Lenz RW. Macromolecules 1992;25:5060–8.
[12] Pardey R, Shen D, Gabori PA, Harris FW, Cheng SZD, Adduci J, Facinelli JV, Lenz RW. Macromolecules 1993;26:3687–97.
[13] Pardey R, Wu SS, Chen J, Harris FW, Cheng SZD, Keller A, Aducci J, Facinelli JV, Lenz RW. Macromolecules 1994;27:5794–802.
[14] Kim SO, Kim TK, Chung IJ. Polymer 2000;41:4709–17.
[15] Kim TK, Kim SO, Chung IJ. Polym Adv Technol 1997;8:305–18.
[16] Chang S, Han CD. Macromolecules 1996;29:2383–91.
[17] Watanabe J, Krigbaum WR. Macromolecules 1984;17:2288–95.
[18] Percec V, Yourd R. Macromolecules 1989;22:524–37.
[19] Percec V, Tsuda Y. Macromolecules 1990;23:5–12.
[20] Percec V, Tsuda Y. Macromolecules 1990;23:3509–20.
[21] Kricheldorf HR, Pakull R, Buchner S. J Polym Sci: Polym Chem 1989;27:431–46.
[22] Kim TK, Kim KM, Chung IJ. Polym J 1997;29:85–94.
[23] Kalika DS, Shen MR, Yu XM, Denn, Iannelli P, Masciocchi N, Yoon DY, Parrish W, Friedrich C, Noel C. Macromolecules 1990;23:5192–200.
[24] Smyth G, Valles EM, Pollack SK, Grebowicz J, Stenhouse PJ, Hsu SL, MacKnight WJ. Macromolecules 1990;23:3389–98.
[25] Cheng SZD, Yandrasits MA, Percec V. Polymer 1991;32:1284–92.
[26] Papadimitrakopoulos F, Hsu SL, MacKnight WJ. Macromolecules 1992;25:4671–81.
[27] Heberer D, Keller A, Percec V. J Polym Sci 1995;33:1877–94.
[28] Ungar G, Feijoo JL, Keller A, Yourd R, Percec V. Macromolecules 1990;23:3411–6.
[29] Fujishiro K, Lenz RW. Macromolecules 1992;25:81–7.
[30] Yandrasits MA, Cheng SZD, Zhang A, Cheng J, Wunderlich B, Percec V. Macromolecules 1992;25:2112–21.
[31] Cheng YY, Cebe P, Gibson HS, Bluhm A, Yeomans W. Macromolecules 1994;27:5440–8.
[32] Lee JB, Kato T, Ujiie S, Iimura K, Uryu T. Macromolecules 1995;28:2165–71.
[33] Cheng YY, Cebe P, Capel M, Gibson HS, Bluhm A, Yeomans W. J Polym Sci 1995;33:2331–41.
[34] Wunder SL, Ramachandran S, Gochanour CR, Weinberg M. Macromolecules 1986;19:1696–702.
[35] Blumstein A, Thomas O, Kumar S. J Polym Sci 1986;24:27–38.
[36] Kim SS, Han CD. Polymer 1994;35:93–103.
[37] Chang S, Han CD. Macromolecules 1997;30:1656–69.
[38] Chang S, Han CD. Macromolecules 1997;30:2021–34.
[39] Gillmor JR, Colby RH, Hall E, Ober CK. J Rheol 1994;38:1623–38.
[40] Keller A, Cheng SZD. Polymer 1998;39:4461–87.
[41] Cheng SZD, Keller A. Annu Rev Mater Sci 1998;28:533–62.
[42] Blumstein A, Thomas O. Macromolecules 1982;15:1264–7.